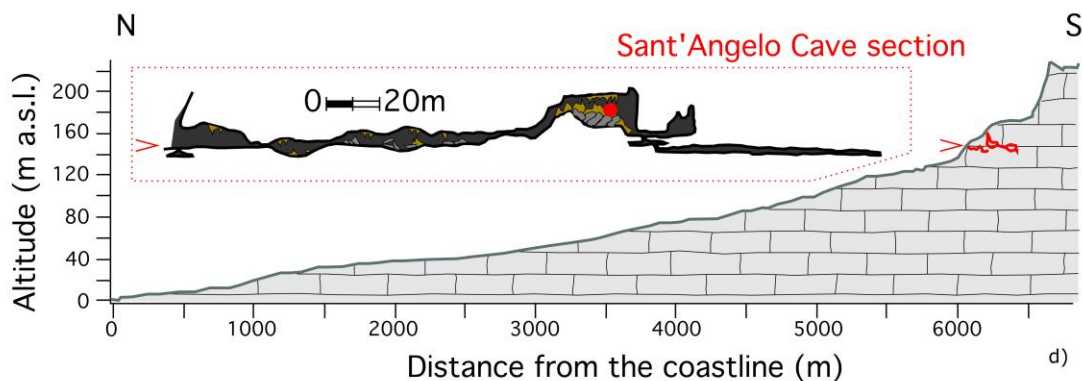
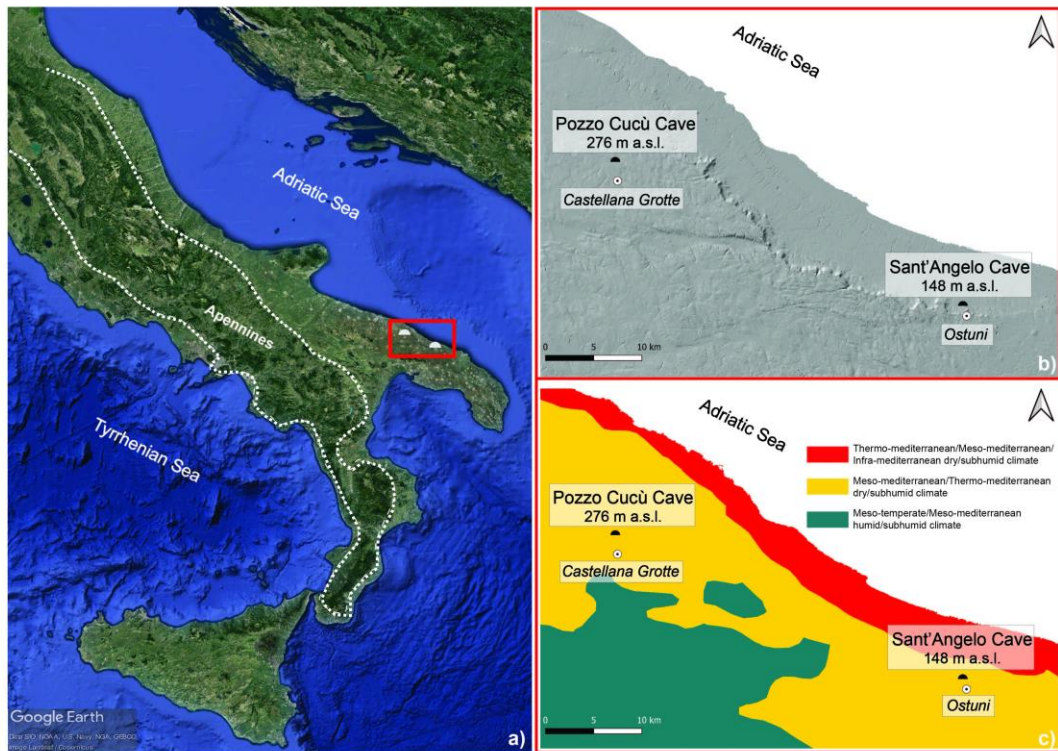


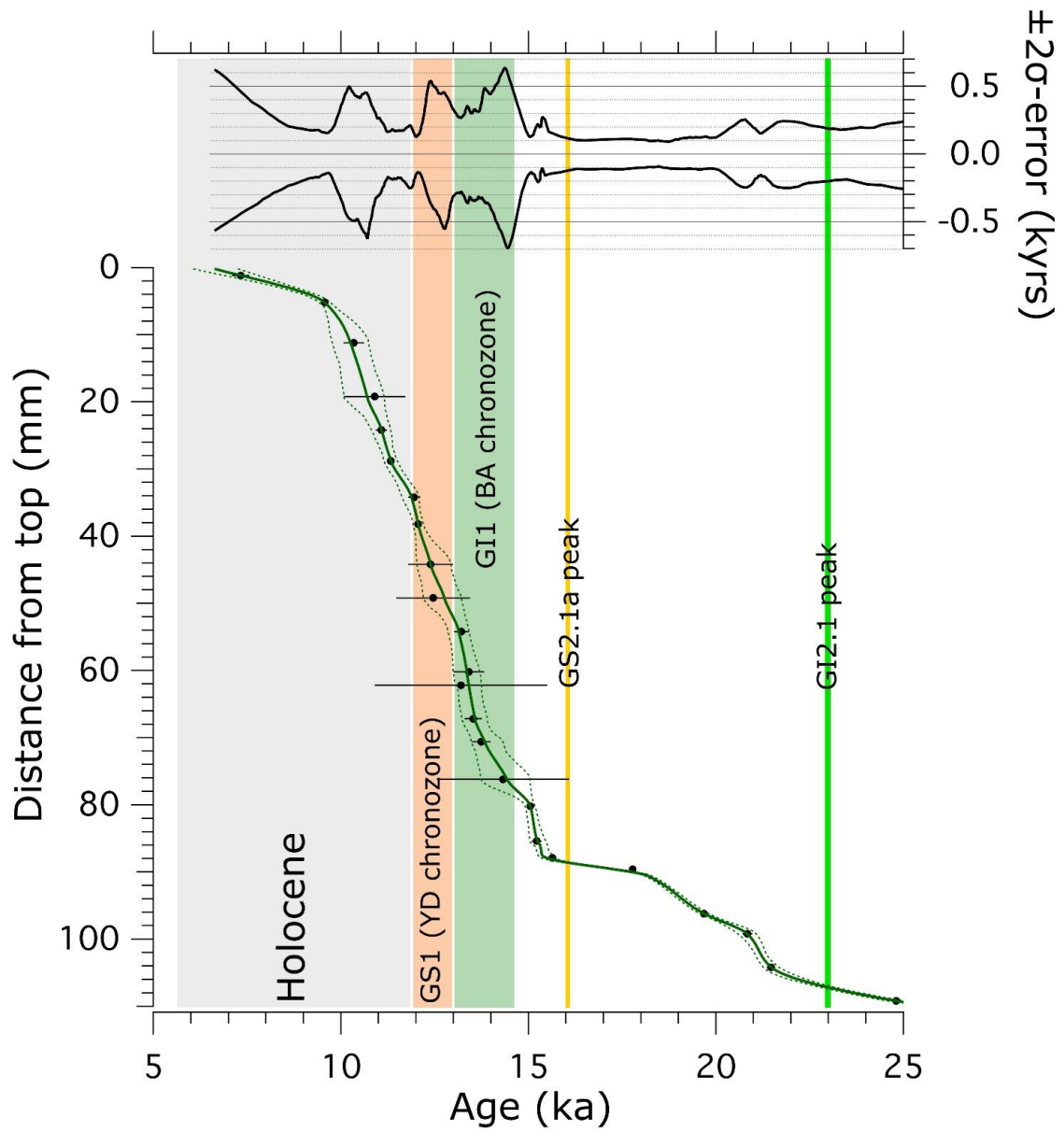
1 **Supplementary**

2  
3



4 **Supplementary figure 1. Study area.** A) Study site (red rectangle) in Apulia,  
5 distant from the Apennine mountain range (dotted line). B) The red rectangle of  
6 (A) is enlarged here, showing the location of Sant'Angelo Cave (this study) and  
7 Pozzo Cucù<sup>1</sup>. The digital elevation model shows that the two caves are located in  
8 a similar topographic setting. C) The same as (B) but showing the climatic micro-  
9 zonation of the area. D) Sant'Angelo Cave profile. SA1 sampling location is  
10 highlighted by the red dot. Cave map and geological section are from D'Angeli et  
11 al (in prep.).

12  
13  
14

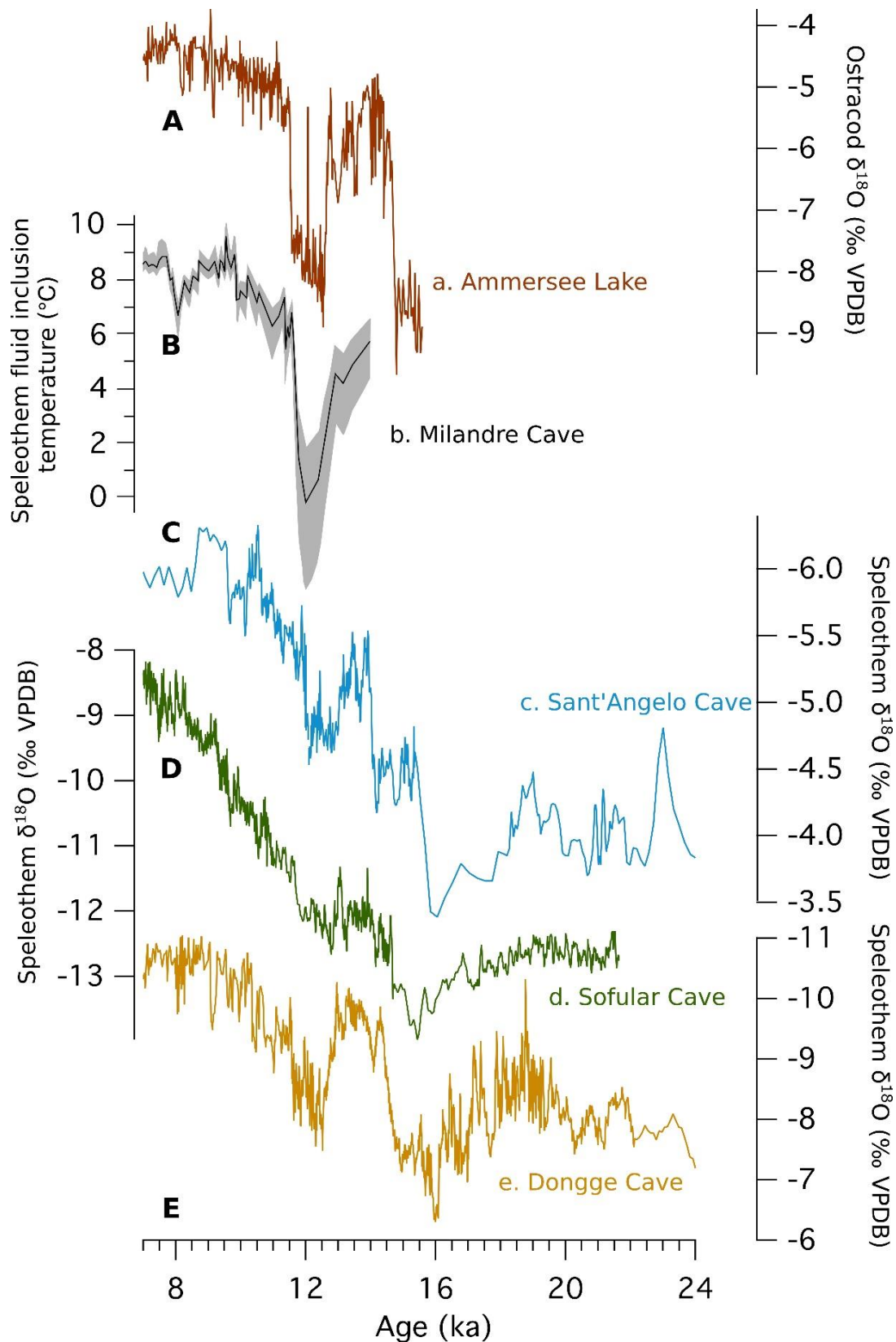


15

16 **Supplementary figure 2.** Age model for the period of interest of this study (~25-  
 17 10 ka). Dots with error bars represent U-Th ages. The solid line is the mean age  
 18 model, and the dotted lines mark the uncertainty envelope. The uncertainties are  
 19 also shown on the graph above, where 2-σ errors are plotted against time.

20

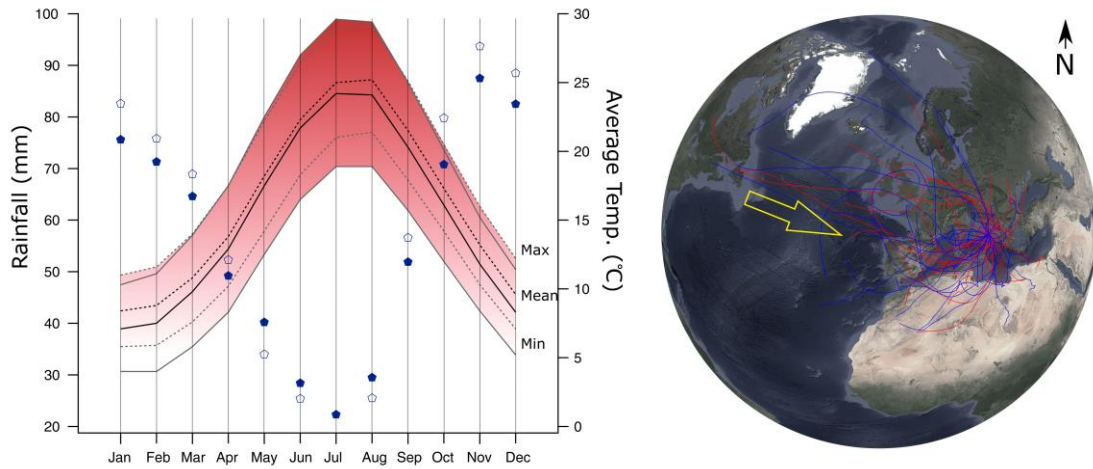
21



22  
23  
24  
25  
26  
27

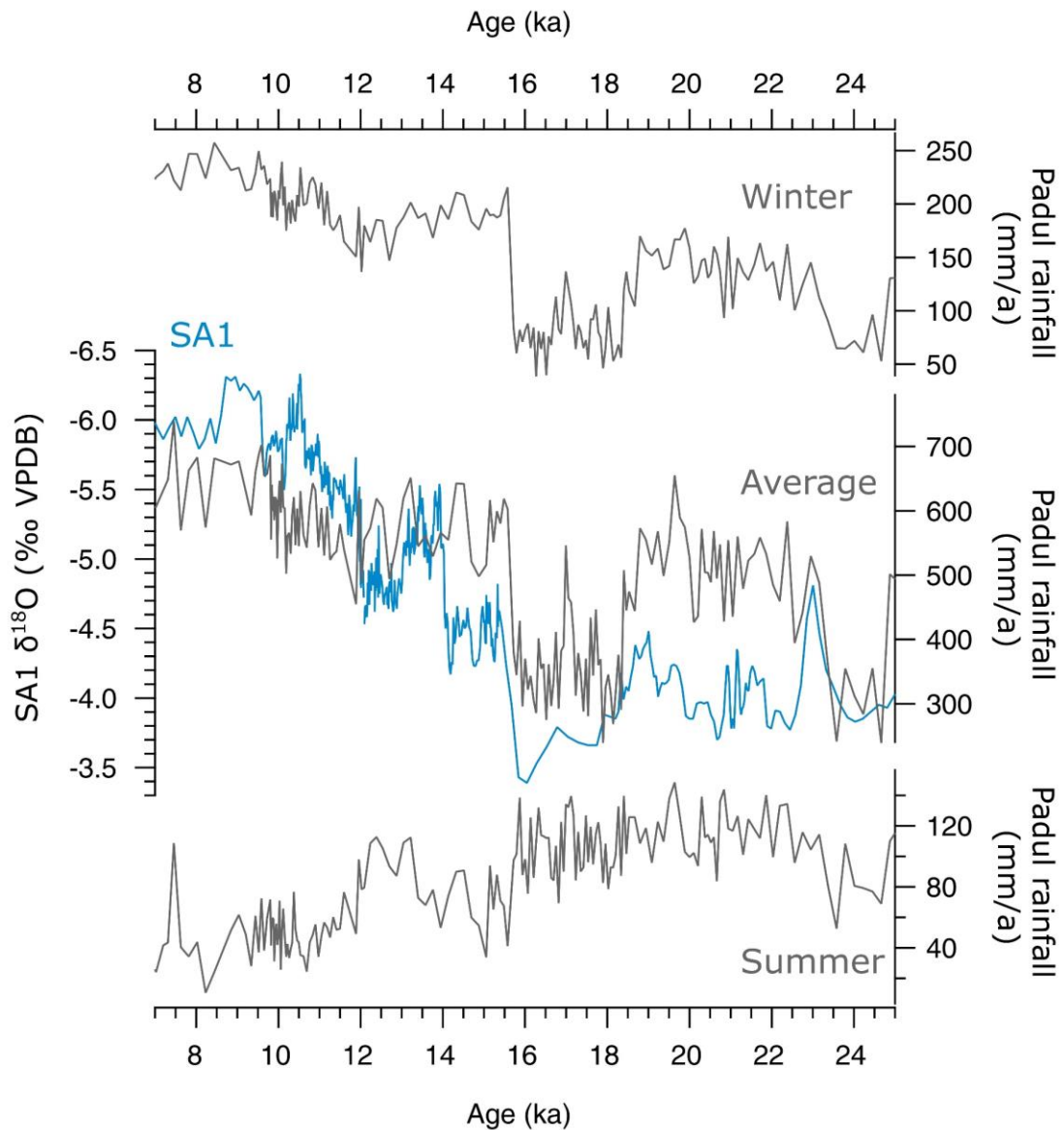
**Supplementary figure 3.** SA1  $\delta^{18}\text{O}$  time series compared to regional records. A) Ammersee Lake<sup>2</sup> (Germany); B) Milandre Cave<sup>3</sup> (Switzerland); C) this study; D) Sofular Cave<sup>4</sup> (Turkey); E) Dongge Cave<sup>5</sup> (China).

28  
29  
30



31  
32

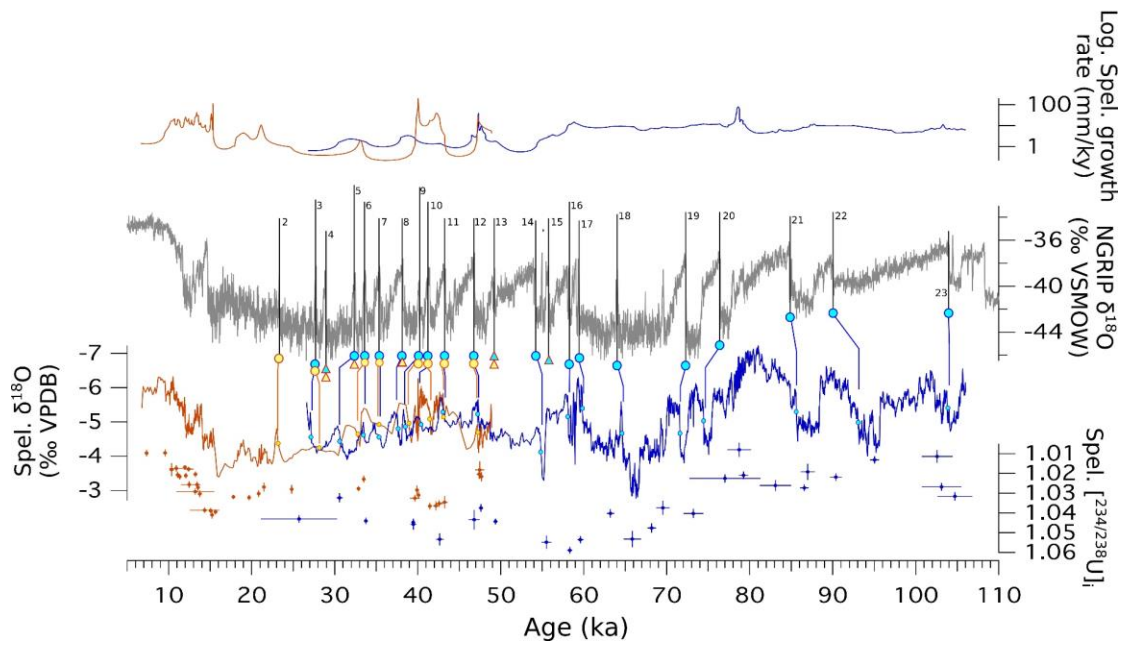
33 **Supplementary figure 4.** Average rainfall and temperature over the last 50 years  
34 (left) based on data from the meteorological station of Ostuni (the nearest with respect to Sant'Angelo Cave) and Castellana Grotte (the nearest with respect to  
35 Pozzo Cucù Cave). Diamonds represent average monthly rainfall, while lines  
36 indicate minimum, average and maximum monthly temperatures. Open diamonds  
37 and dotted lines are for Castellana, while Ostuni is represented by full diamonds  
38 and full lines, On the right, air mass back trajectories were reconstructed using the  
39 Hybrid Single-Particle Lagrangian Integrated Trajectory model (HYSPLIT,  
40 [www.arl.noaa.gov](http://www.arl.noaa.gov)). Simulations were obtained for all 34 rainfall events in 2019.  
41 The current main moisture source of the study area is the Atlantic Ocean (yellow  
42 arrow). Blue and red lines mark air masses at 3015 m and 1500 m a.s.l.,  
43 respectively. Globe map from Google Earth.  
44  
45



46  
47  
48  
49  
50

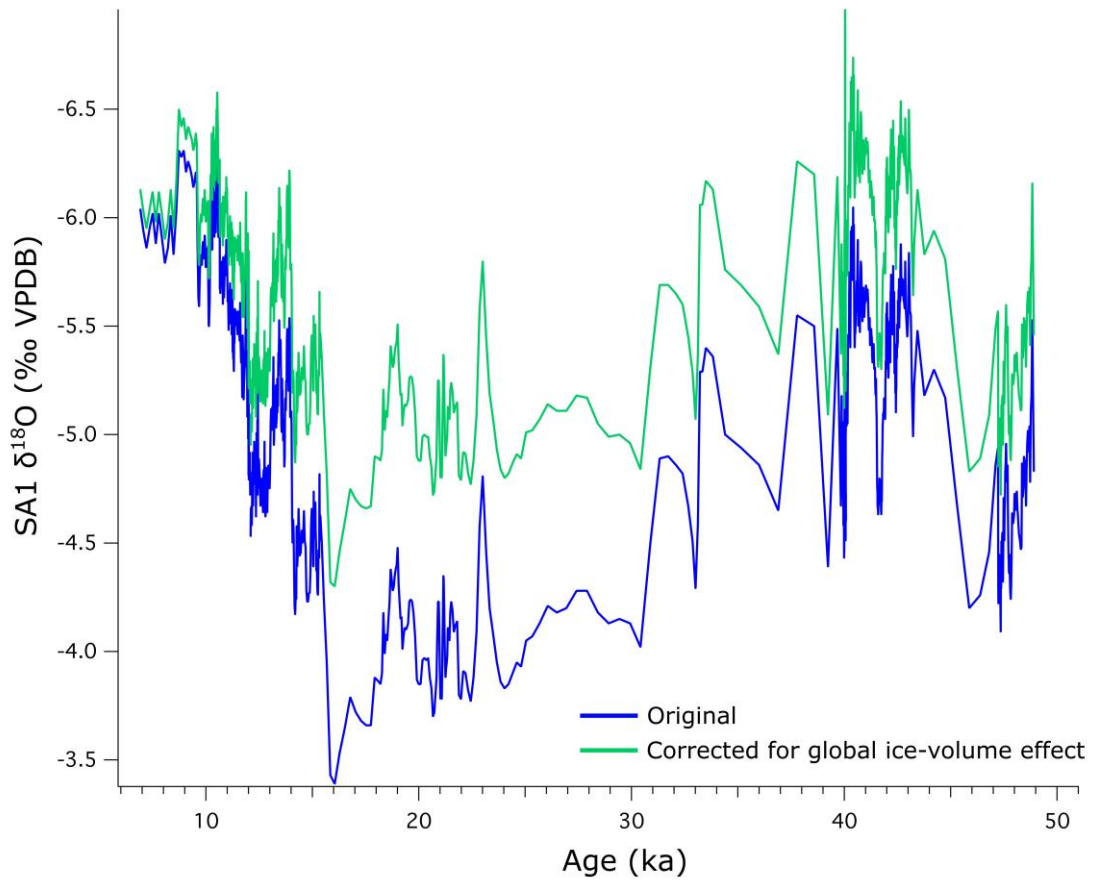
**Supplementary figure 5.** Comparison between SA1 rainfall proxy and reconstructed summer, winter and average rainfall amount from Padul wetland, southern Iberia<sup>6</sup>.





51  
52  
53  
54  
55  
56  
57  
58  
59  
60  
61

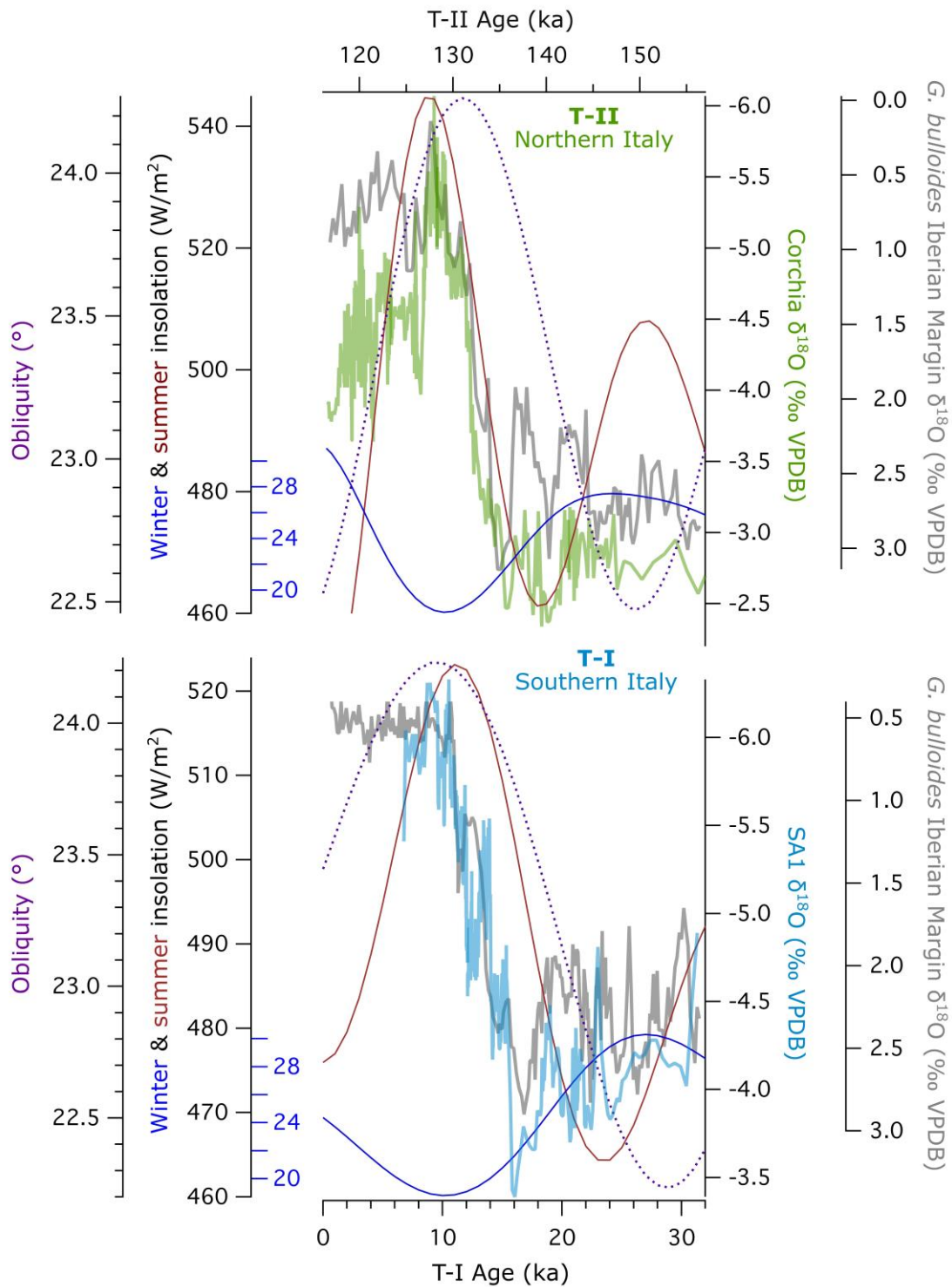
**Supplementary figure 6.** Replication test considering SA1- $\delta^{18}\text{O}$  (orange) and PC- $\delta^{18}\text{O}$  (blue)<sup>1</sup>. Numbered black lines in the Greenland  $\delta^{18}\text{O}$  curve (grey<sup>7</sup>) represent the start of interstadials related to DO cyclicity<sup>8</sup>. Circles mark DOs identified in SA1- $\delta^{18}\text{O}$  (yellow) and PC- $\delta^{18}\text{O}$  (light blue) using the detection algorithm (*methods*); orange and blue lines point to the detected DO in SA1- $\delta^{18}\text{O}$  and PC- $\delta^{18}\text{O}$ , respectively. Triangles mark DOs not detected by the algorithm. The graph also shows growth rates of SA1 and PC (upper portion) and  $[\text{}^{234}/\text{}^{238}\text{U}]_i$ .



62  
63

64 **Supplementary figure 7.** SA1-δ<sup>18</sup>O original data (blue) and corrected for the ice-  
65 volume effect (green, following ref<sup>9</sup>).

66



67  
 68  
 69  
 70  
 71  
 72  
 73  
 74  
 75  
 76

**Supplementary figure 8.** Comparison between T-I in southern Italy (this study, light blue line) and T-II in northern Italy (Corchia Cave<sup>10</sup>) (green line). Both records are compared to planktonic foraminifera (*G. bulloides*) data from the Iberian Margin<sup>11</sup>, as well as obliquity (dotted lines) and winter (blue lines) and summer (brown lines) orbital parameters<sup>12</sup>.

**References**



- 77 <sup>1</sup> Columbu, A., Chiarini, V., Spötl, C., Benazzi, S., Hellstrom, J., Cheng, H., and De  
78 Waele, J., 2020, Speleothem record attests to stable environmental  
79 conditions during Neanderthal-Modern Human turnover in Southern Italy:  
80 Nature Ecology & Evolution, v. 4, no. 9, p. 1188-1195.
- 81 <sup>2</sup> von Grafenstein, U., Erlenkeuser, H., Brauer, A., Jouzel, J., and Johnsen, S. J., 1999,  
82 A mid-European decadal isotope-climate record from 15,500 to 5000 years  
83 BP: Science, v. 284, no. 5420, p. 1654-1657.
- 84 <sup>3</sup> Affolter, S., Häuselmann, A., Fleitmann, D., Edwards, R.L., Cheng, H., and  
85 Leuenberger, M., 2019, Central Europe temperature constrained by  
86 speleothem fluid inclusion water isotopes over the past 14,000 years:  
87 Science Advances, v. 5, no. 6.
- 88 <sup>4</sup> Badertscher, S., Fleitmann, D., Cheng, H., Edwards, R. L., Göktürk, O. M., Zumbühl,  
89 A., Leuenberger, M., and Tüysüz, O., 2011, Pleistocene water intrusions  
90 from the Mediterranean and Caspian seas into the Black Sea: Nature  
91 Geoscience, v. 4, no. 4, p. 236-239.
- 92 <sup>5</sup> Cheng, H., Zhang, P. Z., Spötl, C., Edwards, L., Cai, Y. J., Zhang, D. Z., Sang, W. C., Tan,  
93 M., and An, Z. S., 2012, The climatic cyclicity in semiarid - arid central Asia  
94 over the past 500,000 years: Geophysical Research Letters, v. 39, no. 1.
- 95 <sup>6</sup> Camuera, J., Ramos-Román, M., Jiménez-Moreno, G., García-Alix, A., Ilvonen, L.,  
96 Ruha, L., Gil-Romera, G., González-Sampériz, P., and Seppä, H., 2022.  
97 Quantitative reconstruction of hydroclimate variability over the last 200  
98 kyr in the West Mediterranean. PANGAEA,  
99 <https://doi.org/10.1594/PANGAEA.940006>
- 100 <sup>7</sup> North Greenland Ice Core Project (NGRIP) Members, 2004, High-resolution  
101 record of Northern Hemisphere climate extending into the last interglacial  
102 period: Nature, v. 431, no. 7005, p. 147-151.
- 103 <sup>8</sup> Rasmussen, S. O., Bigler, M., Blockley, S. P., Blunier, T., Buchardt, S. L., Clausen, H.  
104 B., Cvijanovic, I., Dahl-Jensen, D., Johnsen, S. J., Fischer, H., Gkinis, V.,  
105 Guillevic, M., Hoek, W. Z., Lowe, J. J., Pedro, J. B., Popp, T., Seierstad, I. K.,  
106 Steffensen, J. P., Svensson, A. M., Vallelonga, P., Vinther, B. M., Walker, M. J.  
107 C., Wheatley, J. J., and Winstrup, M., 2014, A stratigraphic framework for  
108 abrupt climatic changes during the Last Glacial period based on three  
109 synchronized Greenland ice-core records: refining and extending the  
110 INTIMATE event stratigraphy: Quaternary Science Reviews, v. 106, p. 14-  
111 28.
- 112 <sup>9</sup> Bintanja, R., van de Wal, R. S., and Oerlemans, J., 2005, Modelled atmospheric  
113 temperatures and global sea levels over the past million years: Nature, v.  
114 437, p. 125-128.
- 115 <sup>10</sup> Drysdale, R. N., Hellstrom, J. C., Zanchetta, G., Fallick, A. E., Sanchez Goni, M. F.,  
116 Couchoud, I., McDonald, J., Maas, R., Lohmann, G., and Isola, I., 2009,  
117 Evidence for obliquity forcing of glacial Termination II: Science, v. 325, no.  
118 5947, p. 1527-1531.
- 119 <sup>11</sup> Martrat, B., Grimalt, J. O., Shackleton, N. J., de Abreu, L., Hutterli, M. A., and  
120 Stocker, T. F., 2007, Four climate cycles of recurring deep and surface water  
121 destabilizations on the Iberian margin: Science, v. 317, no. 5837, p. 502-  
122 507.
- 123 <sup>12</sup> Berger, A. and Loutre, M. F., 1991, Insolation values for the climate of the last 10  
124 million years. Quaternary Science Reviews, v. 10, p. 297-317.